DOA and Phase Error Estimation for a Partly Calibrated Array With Arbitrary Geometry

XUEJING ZHANG , Student Member, IEEE
ZISHU HE , Member, IEEE
University of Electronic Science and Technology of China, Chengdu, China

XUEPAN ZHANG
Qian Xuesen Laboratory of Space Technology, Beijing, China

YUE YANG, Student Member, IEEE
University of Electronic Science and Technology of China, Chengdu, China

This paper presents a novel strategy to simultaneously estimate the direction of arrival (DOA) of a source signal and the phase error of a partly calibrated array with arbitrary geometry. We add up the snapshot data of two different sensors, and then extract a knowledge associated with the DOA and phase errors of these two elements by using singular value decomposition. In such a manner, we can establish a series of linear equations with respect to the unknown DOA and phase error, by simply conducting the procedure on any two sensor elements. On this basis, it can be shown that the problem of jointly estimating DOA and phase error is equivalent to a least square (LS) problem with a quadratic equality constraint. To solve this LS problem (so that the DOA and phase error can be obtained), an effective convex–concave procedure is employed. Different from the conventional algorithms that are limited to specific array geometries, the proposed one is suitable for arrays with arbitrary geometries. More importantly, the devised method only requires one extra calibrated sensor, which is not necessarily adjacently located with the reference one. Several simulations are carried out in this paper and the effectiveness of the devised method can be clearly observed.

Manuscript received November 28, 2017; revised April 20, 2018, August 30, 2018, and December 1, 2018; released for publication April 22, 2019. Date of publication May 8, 2019; date of current version February 7, 2020.

DOI. No. 10.1109/TAES.2019.2915422

Refereeing of this contribution was handled by H. Mir.

This work was supported in part by the National Natural Science Foundation of China under Grant 61671139, Grant 61671137, Grant 61701499, and Grant 61871085; in part by the Fundamental Research Funds for the Central Universities under Grant 2672018ZYGX2018J010; and in part by the China Scholarship Council. This paper was presented in part at the 24th European Signal Processing Conference, Budapest, Hungary, August/September 2016.

Authors' addresses: Xuejing Zhang, Z. He, and Y. Yang are with the University of Electronic Science and Technology of China, Chengdu 611731, China, E-mail: (xjzhang7@163.com; zshe@uestc.edu.cn; yueyang@std.uestc.edu.cn); Xuepan Zhang is with the Qian Xuesen Laboratory of Space Technology, Beijing 100094, China, E-mail: (zhangxuepan@qxslab.cn), *(Corresponding author: Xuejing Zhang.)*

I. INTRODUCTION

Array signal processing has been extensively applied in the fields like radar, navigation, wireless communication, and so forth. One of the most important topics in array processing is direction-of-arrival (DOA) estimation [1]–[6], in which the DOAs of plane waves impinging on a sensor array need to be determined. Many high-resolution eigendecomposition methods such as multiple signal classification (MUSIC) [7], estimation of signal parameter via rotational invariance technique (ESPRIT) [8], and maximum likelihood (ML) [9] have been devised to tackle the problem of DOA estimation. However, it has been generally accepted that the performance of these methods is critically dependent on the knowledge of the array manifold. Unfortunately, the array perturbations are inevitable in practical applications, and hence the estimators performance would degrade substantially when errors exist and the assumed observation model deviates from real situation.

Many efforts have been devoted to DOA estimation when an array suffers from unexpected perturbations [10]–[19]. In particular, Friedlander and Weiss proposed an alternative iterative method (named as WF method) [20], which is able to estimate the DOAs and gain–phase error of each sensor element simultaneously. However, this method may be considerably deteriorated in the presence of large phase uncertainties. The eigenstructure based methods in [21] and [22] perform well especially when the phase error is large. However, both of these two methods require two calibration signals to estimate the unknown parameters. Boon Chong and Chong Meng Samson [23] have developed a calibration approach by taking advantage of the ML theory. However, it suffers from heavy computational load and requires a set of calibration sources in known locations. A phase retrieval based method is reported in [24] to estimate DOAs and array errors, when multiple signals exist. By modeling the array perturbations as random parameters, a maximum *a posteriori* approach is proposed in [25] to estimate these perturbations. This algorithm is able to calibrate the sensor array in an automatic way, but it requires knowledge of the second-order statistics of the perturbation parameters. A subspace method for estimating array gains and phases is proposed in [26], and a satisfactory performance can be obtained if the angles of DOAs are known. A practical calibration technique is developed in [27], by using the MUSIC null spectrum property. This method is applicable for arbitrary array; however, it achieves desirable performance under the assumption that one or more signal sources are known. A blind signal separation based DOA estimation and array error calibration method is recently reported in [28], where an inefficient search of two-dimensional (2-D) spatial spectrum is needed.

In addition, there are also several other excellent approaches to array error calibration developed by utilizing the geometry structure of array or the special property of covariance matrix. For example, Paulraj and Kailath [29] estimate gain/phase error of a uniform linear array (ULA) by taking advantage of the Toeplitz structure of covariance matrix. This method is further modified in [30] with a superior performance and a dramatically reduced complexity. In [31], the problem of DOA estimation in the presence of an unknown phase error of a ULA is addressed, by exploiting the information available in the sample covariance matrix. The partial Toeplitz structure of the covariance matrix is employed in [32] to estimate the model errors of nested sensor arrays. For the above-mentioned methods, their generalizations to arrays with arbitrary geometries cannot be easily extended.

Recently, partly calibrated arrays [33]–[35] have received great research interests. A partly calibrated array assumes that some sensor elements have been perfectly calibrated, whereas others remain uncalibrated. It has been shown in [36] that if each subarray is calibrated, a spectral rank-reduction algorithm can be utilized to determine the DOAs. By exploiting the principle of conventional ESPRIT scheme, a computationally efficient ESPRIT-like algorithm is devised in [37], where the DOAs as well as the unknown gains and phases in the uncalibrated portion of the array can be simultaneously estimated using a closed-form expression. In [38], the ESPRIT-like algorithm is further investigated. More specifically, the identifiability of DOA estimation is addressed in detail and a refining scheme is proposed to improve the performance. Besides, the ESPRIT-like algorithm has been recently extended in [39] to the scenario of nonuniform noise circumstance. It should be noted that the above approaches in [36]–[39] require at least one pair of consecutive calibrated sensors. Moreover, the ESPRIT-like algorithm is limited to ULAs, and its generalization to other array configurations is not well considered.

To overcome the imperfections of the above algorithms, a new method is presented in this paper to jointly estimate the DOA and phase error of a partly calibrated array with arbitrary geometry. The proposed method is able to estimate the DOA of a single signal as well as the phase errors of array elements, by using one calibrated sensor that is different from the reference one. This paper was previously presented in part in [1]; we extend the preliminary work by modifying the algorithm and enriching the simulations. More specifically, the devised approach is developed on the basis of the well-known Euler's formula. Analysis shows that the summation of snapshot data of two different sensor elements provides knowledge about the DOA of the single source and the phase errors of corresponding sensors. Based on this observation, we establish a least square (LS) problem with a quadratic equality constraint, by adding up snapshot data of any two elements and then carrying out a singular value decomposition (SVD) procedure. We recover the DOA and phase errors simultaneously by solving the LS problem with the convex–concave procedure (CCP) [40], which is more efficient than the previous generalized singular value decomposition (GSVD) approach in [1] and results a better performance than the semidefinite relaxation (SDR) approach in the same reference. Different from the conventional algorithms that are limited to specific array configurations, the proposed one is suitable for arrays with arbitrary geometries. More importantly, the devised method only requires one extra calibrated sensor, which is not necessarily adjacently located with the reference one. It should be noted that our method is still applicable if multiple sensors were calibrated. Moreover, for a fully uncalibrated array, the proposed method also works after simple modifications as detailed later. In addition, the single source can be a noncooperative source whose angle needs to be estimated or a calibration source (whose angle is also not precisely known) assigned to calibrate the array. In the latter case, we can first calibrate the array using the single source, and then apply the calibrated array to estimate noncooperative source whose number may be greater than one. We should also point out that the proposed algorithm has no ability to calibrate mutual coupling and array shape perturbation. This is a limitation that needs to be addressed in our future study. Various simulations are carried out to illustrate the effectiveness of the devised method under different situations.

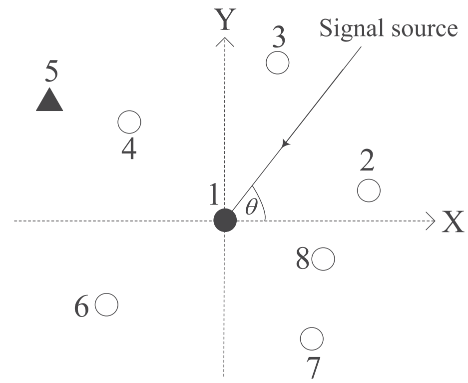

Fig. 1. Illustration of a partly calibrated array (the solid circle denotes the reference sensor and the triangle symbol stands for the calibrated sensor).

The rest of the paper is organized as follows. In Section II, the problem of DOA and phase error estimation for a partly calibrated array is introduced. The proposed algorithm is presented in Section III and the Cramér–Rao bounds (CRBs) are derived in Section IV. Representative simulations are conducted in Section V and conclusions are drawn in Section VI.

II. PROBLEM FORMULATION

Consider a planar array with N omnidirectional sensors. Without loss of generality, we focus on the case that the array and signal source are coplanar, although its extension to more generalized cases is straight forward. It is assumed that one single source impinges on the array from θ (see Fig. 1). Under ideal circumstance, the nominal steering vector $\mathbf{a}(\theta)$ is given by

$$\mathbf{a}(\theta) = [1, e^{j2\pi\lambda^{-1}\mathbf{p}_2^{\mathrm{T}}\mathbf{r}}, \dots, e^{j2\pi\lambda^{-1}\mathbf{p}_N^{\mathrm{T}}\mathbf{r}}]^{\mathrm{T}} \tag{1}$$

where $(\cdot)^{\mathrm{T}}$ denotes the transpose operator, $j = \sqrt{-1}$ is the imaginary unit, $\mathbf{p}_n = [x_n, y_n]^{\mathrm{T}}$ stands for the coordinate of the nth sensor ($n = 1, 2, \dots, N$), and $\mathbf{r} = [\cos(\theta), \sin(\theta)]^{\mathrm{T}}$ is the unit vector corresponding to the direction θ.

Under practical scenario, the phase error exists, and the actual steering vector $\mathbf{a}_r(\theta)$ satisfies

$$\mathbf{a}_r(\theta) = \Gamma\mathbf{a}(\theta) \tag{2}$$

where Γ is the phase error matrix as

$$\Gamma = \mathrm{diag}\{[e^{j\phi_1}, e^{j\phi_2}, \dots, e^{j\phi_N}]\} \tag{3}$$

with ϕ_n denoting the phase error of the nth sensor and $\mathrm{diag}(\cdot)$ returning a diagonal matrix whose diagonal equals the input vector. In this paper, we take the first sensor as the reference one, i.e., $\phi_1 = 0$. Accordingly, the received vector of array can be expressed as

$$\mathbf{x}(t) = \mathbf{a}_r(\theta)s(t) + \mathbf{n}(t) = \Gamma\mathbf{a}(\theta)s(t) + \mathbf{n}(t) \tag{4}$$

where $s(t)$ contains the complex envelope of the signal, and $\mathbf{n}(t)$ is a complex Gaussian white additive $N \times 1$ noise vector. In addition, we assume that

$$E\left\{s(t)s^*(t)\right\} = \sigma_s^2 \tag{5a}$$

$$E\left\{\mathbf{n}(t)\mathbf{n}^{\mathrm{H}}(t)\right\} = \sigma_n^2\mathbf{I} \tag{5b}$$

where σ_s^2 and σ_n^2 stand for the powers of signal and noise, respectively. The snapshot data matrix composed of L snapshots can be written as

$$\mathbf{X} = [\mathbf{x}(1), \mathbf{x}(2), \dots, \mathbf{x}(L)] = \Gamma\mathbf{a}(\theta)\mathbf{S} + \mathbf{N} \tag{6}$$

where $\mathbf{S} = [s(1), \dots, s(L)]$ and $\mathbf{N} = [\mathbf{n}(1), \dots, \mathbf{n}(L)]$. Note that only phase error is considered in the above model. In some cases, there also exists gain error among sensor array elements. Under this circumstance, the actual steering vector is given by $\mathbf{a}_r(\theta) = \mathbf{G}\Gamma\mathbf{a}(\theta)$, where $\mathbf{G}$ is an $N \times N$ diagonal matrix with the nth diagonal element g_n, $n = 1, \dots, N$. As reported in [21], the gain error g_n can be estimated by

$$\hat{g}_n = \sqrt{\frac{\mathbf{R}(n, n) - \frac{1}{N-1}\sum_{n=2}^{N}\rho_n}{\mathbf{R}(1, 1) - \frac{1}{N-1}\sum_{n=2}^{N}\rho_n}} \tag{7}$$

where $\mathbf{R}$ stands for the covariance matrix that can be estimated using the snapshot data $\mathbf{X}$, ρ_n is the nth eigenvalues of $\mathbf{R}$, $n = 1, \dots, N$. Once $\hat{g}_n$ ($n = 1, \dots, N$) is obtained, we can compensate the gain error and leave only the phase error.

Obviously, the conventional direction finding methods would fail if phase error exists, due to the mismatch between the actual and nominal array manifolds. In this paper, we consider how to estimate DOA and phase error for a partly calibrated array. More specifically, we assume that one sensor (except the reference one) whose label is c has been calibrated. In this case, it can be assumed that ϕ_c is known. Our objective is to jointly estimate the DOA θ and phase error from array output $\mathbf{X}$.

III. PROPOSED METHOD

In this section, the main concept of the proposed method is given by taking advantages of Euler's formula. Then, an effective strategy is provided to improve the practicality of the proposed scheme. We convert the estimation of DOA and phase error into an LS problem with a quadratic equality constraint, and solve the LS problem using the CCP approach.

A. Main Idea of Estimating DOA and Phase Error

Before presenting the details to estimate DOA and phase error of a partly calibrated array, we first give the following formula:

$$e^{jA} + e^{jB} = 2\Re(e^{j\frac{A-B}{2}})e^{j\frac{A+B}{2}} \tag{8}$$

where both A and B are real values, and $\Re(\cdot)$ outputs the real part of the bracketed term. The expression (8) can be readily derived from Euler's formula and plays an important role in our following discussion.

To begin with, let $\mathbf{A}(n, :)$ be the nth row of matrix $\mathbf{A}$. Recalling (6), one easily obtains that

$$\mathbf{X}(n, :) = e^{j(2\pi\lambda^{-1}\mathbf{p}_n^{\mathrm{T}}\mathbf{r}+\phi_n)}\mathbf{S} + \mathbf{N}(n, :). \tag{9}$$

Define $\mathbf{X}_{i+k}$ as the summation of $\mathbf{X}(i, :)$ and $\mathbf{X}(k, :)$, i.e.,

$$\mathbf{X}_{i+k} \triangleq \mathbf{X}(i, :) + \mathbf{X}(k, :). \tag{10}$$

Combining (9) and (10), and utilizing (8), we have

$$\begin{aligned}\mathbf{X}_{i+k} &= \mathbf{X}(i, :) + \mathbf{X}(k, :) \\ &= \left(e^{j(2\pi\lambda^{-1}\mathbf{p}_i^{\mathrm{T}}\mathbf{r}+\phi_i)} + e^{j(2\pi\lambda^{-1}\mathbf{p}_k^{\mathrm{T}}\mathbf{r}+\phi_k)}\right)\mathbf{S} + \mathbf{N}_{i+k} \\ &= c_{i+k}e^{j\Psi_{i+k}}\mathbf{S} + \mathbf{N}_{i+k}\end{aligned} \tag{11}$$

where $\mathbf{N}_{i+k} = \mathbf{N}(i, :) + \mathbf{N}(k, :)$ is the compound noise, c_{i+k} is a real value as

$$c_{i+k} = 2\Re\left(e^{j(\pi\lambda^{-1}(\mathbf{p}_i-\mathbf{p}_k)^{\mathrm{T}}\mathbf{r}+\frac{\phi_i-\phi_k}{2})}\right). \tag{12}$$

The Ψ_{i+k} in (11) relates to the unknown parameters ϕ_i, ϕ_k, and θ, more precisely, it satisfies

$$\Psi_{i+k} = \pi\lambda^{-1}(\mathbf{p}_i + \mathbf{p}_k)^{\mathrm{T}}\mathbf{r} + (\phi_i + \phi_k)/2 = \mathbf{b}_{i+k}^{\mathrm{T}}\mathbf{u} \tag{13}$$

where $\mathbf{u}$ represents the parameter vector as

$$\mathbf{u} = [\phi_1, \phi_2, \dots, \phi_N, \cos(\theta), \sin(\theta)]^{\mathrm{T}} \in \mathbb{R}^{N+2}. \tag{14}$$

$$\begin{aligned}\mathbf{b}_{i+k} = [&0, \dots, 0, 1/2, 0, \dots, 0, 1/2, 0, \dots, 0, \pi\lambda^{-1}x_n, \\ &\pi\lambda^{-1}y_n]^{\mathrm{T}} \in \mathbb{R}^{N+2}\end{aligned} \tag{15}$$

$\mathbf{b}_{i+k}$ in (13) is the corresponding coefficient vector as. Notice that in $\mathbf{b}_{i+k}$, the ith and the kth elements are $1/2$, and the last two entries are $\pi\lambda^{-1}x_n$ and $\pi\lambda^{-1}y_n$, respectively.

According to (13), we know that Ψ_{i+k} is a linear combination of the phase errors (i.e., ϕ_i and ϕ_k) and two mappings of DOA (i.e., $\cos(\theta)$ and $\sin(\theta)$). Based on this fact, it is possible to recover the unknown phase error and DOA by exploiting the knowledge of Ψ_{i+k}.

To obtain an estimation of Ψ_{i+k}, we construct $\mathbf{Y}_{i+k}$ as

$$\mathbf{Y}_{i+k} = \begin{bmatrix} \mathbf{X}(1,:) \\ \mathbf{X}_{i+k} \end{bmatrix} = \begin{bmatrix} 1 \\ c_{i+k}e^{j\Psi_{i+k}} \end{bmatrix}\mathbf{S} + \begin{bmatrix} \mathbf{N}(1,:) \\ \mathbf{N}_{i+k} \end{bmatrix}. \quad (16)$$

According to the subspace principle, the following equality can be established:

$$\operatorname{span}\left(\begin{bmatrix} 1 \\ c_{i+k}e^{j\Psi_{i+k}} \end{bmatrix}\right) = \operatorname{span}(\boldsymbol{\gamma}_{i+k}) \quad (17)$$

where $\operatorname{span}(\cdot)$ returns the range space of the input matrix, and $\boldsymbol{\gamma}_{i+k}$ is the principal left singular vector of $\mathbf{Y}_{i+k}$. More specifically, $\boldsymbol{\gamma}_{i+k}$ can be obtained with the help of SVD of $\mathbf{Y}_{i+k}$ as

$$\mathbf{Y}_{i+k} = \underbrace{[\boldsymbol{\gamma}_{i+k}, \mathbf{U}_2]}_{\mathbf{U}}\boldsymbol{\Sigma}\mathbf{V}^{\mathrm{H}} \quad (18)$$

where $\mathbf{U}$ and $\mathbf{V}$ denote the left singular vectors and right singular vectors of $\mathbf{Y}_{i+k}$, respectively. Assuming that the first entry of $\boldsymbol{\gamma}_{i+k}$ has been normalized to one, it can be readily obtained from (17) that

$$c_{i+k}e^{j\Psi_{i+k}} = \boldsymbol{\gamma}_{i+k}(2) \quad (19)$$

where $\boldsymbol{\gamma}_{i+k}(2)$ stands for the second entry of $\boldsymbol{\gamma}_{i+k}$. The expression (19) is an essential formulation for the analysis next.

Note that c_{i+k} in (19) may be either positive or negative. Moreover, Ψ_{i+k} may locate beyond the range of $[0, 2\pi]$. Therefore, if no prior knowledge of the sign of c_{i+k} or a rough estimation of Ψ_{i+k} is available, the Ψ_{i+k} cannot be accurately estimated. Fortunately, provided that

$$\operatorname{abs}(\Psi_{i+k}) \leq \pi/2 \quad (20)$$

one derives from (19) that

$$\Psi_{i+k} = \mathbf{b}_{i+k}^{\mathrm{T}}\mathbf{u} = \angle(\boldsymbol{\gamma}_{i+k}(2)) \triangleq \operatorname{atan}\left(\frac{\Im(\boldsymbol{\gamma}_{i+k}(2))}{\Re(\boldsymbol{\gamma}_{i+k}(2))}\right) \quad (21)$$

where $\angle(\cdot)$ returns the (principal) argument of the input complex number and its definition has been implicitly given on the right-hand side of (21). Since the resulting Ψ_{i+k} in (21) locates in $[-\pi/2, \pi/2]$, a correct estimation of Ψ_{i+k} can thus be obtained. From the above discussion, we know that if (20) holds true, (21) provides a measurement of ϕ_i, ϕ_k, and θ, with a specific weighting coefficient $\mathbf{b}_{i+k}$.

Recalling the assumed setting for a partly calibrated array (i.e., $\phi_1 = 0$ and ϕ_c is known *a priori*), (21) can be rearranged as

$$\mathbf{w}_{i+k}^{\mathrm{T}}\mathbf{v} = \angle[\boldsymbol{\gamma}_{i+k}(2)] - \phi_c\mathbf{b}(c) \quad (22)$$

where $\mathbf{v} = [\phi_2, \ldots, \phi_{c-1}, \phi_{c+1}, \ldots, \phi_N, \cos(\theta), \sin(\theta)]^{\mathrm{T}}$ is a modified parameter vector by removing ϕ_1 and ϕ_c from $\mathbf{u}$, and $\mathbf{w}_{i+k}$ is similarly obtained by removing the corresponding terms from $\mathbf{b}_{i+k}$.

To summarize, by taking various of pairs of i and k (satisfying $i, k = 1, 2, \ldots, N$ and $i \neq k$), a series of linear equations [i.e., (22)] with respect to the unknown parameters can be obtained. Therefore, if we can obtain enough equations, it is possible to determine all the unknown parameters. To have an intuitive perspective of the proposed scheme, an illustration of the devised strategy is demonstrated in Fig. 2, from which the proposed method can be clearly understood.

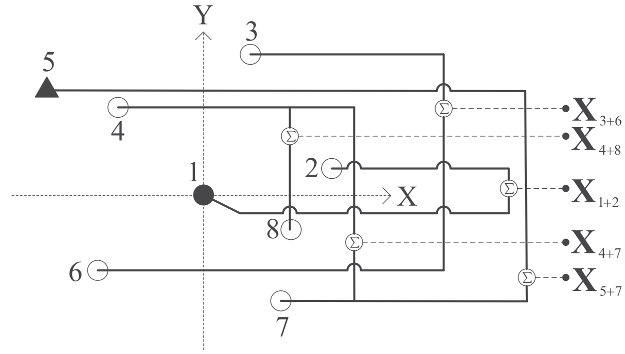

Fig. 2. Illustration of the proposed scheme.

However, notice again that the linear equation of (21) or (22) is developed on the precondition of (20), which is not easily satisfied in practice. In other words, there may be only quite a few portion of pairs of i and k happened to meet condition (20). As a consequence, it would result in an underdetermined problem, which gives innumerable solutions. To handle this difficulty, we introduce a useful method in the following section. Using this strategy, the practicality of the proposed scheme can be greatly improved.

REMARK 1 Note that if there exists an additional mutual coupling error between sensor elements, the above discussion will not be true any longer. To see this point, we denote by $\mathbf{C} \in \mathbb{C}^{N \times N}$ the mutual coupling matrix. In this case, the actual steering vector $\mathbf{a}_r(\theta)$ satisfies

$$\mathbf{a}_r(\theta) = \mathbf{C}\Gamma\mathbf{a}(\theta).$$

Since $\mathbf{C}$ is complex symmetry with unit elements on diagonal, we can readily express the nth entry of $\mathbf{a}_r(\theta)$ (denoted by $[\mathbf{a}_r(\theta)]_n$) as

$$[\mathbf{a}_r(\theta)]_n = e^{j(2\pi\lambda^{-1}\mathbf{p}_n^{\mathrm{T}}\mathbf{r}+\phi_n)} + \sum_{l=1,l\neq n}^{N}\mathbf{C}(n,l)e^{j(2\pi\lambda^{-1}\mathbf{p}_l^{\mathrm{T}}\mathbf{r}+\phi_l)}$$

where $\mathbf{C}(n, j)$ represents the nth row and the jth column element of $\mathbf{C}$. On this basis, it is not hard to obtain that

$$\mathbf{X}_{i+k} = \mathbf{X}(i,:) + \mathbf{X}(k,:) = (c_{i+k}e^{j\Psi_{i+k}} + \epsilon_{i+k})\mathbf{S} + \mathbf{N}_{i+k}$$

where an additional bias ϵ_{i+k} (its value depends on $\mathbf{C}(i,:)$, $\mathbf{C}(k,:)$, and Γ) is incorporated compared to (11). Then according to the subspace principle, we can obtain an estimate of $\angle(c_{i+k}e^{j\Psi_{i+k}} + \epsilon_{i+k})$, but not the phase Ψ_{i+k} as derived in (21). As a result, the mutual coupling seriously degrades the performance of our method. One can apply the array interpolation methods in [16]–[19] to realize the calibration under this circumstance, by deploying additional sources.

B. Method to Improve Practicality

Before proceeding, it is reasonably assumed that ϕ_n $(n = 1, 2, \ldots, N)$ is zero mean and uniformly distributed in the range $[-\Delta, \Delta]$. More clearly, ϕ_n satisfies

$$\phi_n \in [-\Delta, \Delta]. \tag{23}$$

Additionally, we suppose that the DOA of the source signal locates in the set $\mathcal{D}$ as

$$\mathcal{D} = \left\{\theta \middle| \theta_0 - \delta_\theta \leq \theta \leq \theta_0 + \delta_\theta\right\} \tag{24}$$

where θ_0 is a coarse estimation of the DOA that can be easily obtained by using a conventional direction finding method such as Capon beamforming [41]; δ_θ in (24) describes the perturbation of the DOA estimation.

Instead of dealing with Ψ_{i+k} directly, here we define a shifted version of Ψ_{i+k} as

$$\widetilde{\Psi}_{i+k} \triangleq \Psi_{i+k} - C_{i+k} \tag{25}$$

where C_{i+k} stands for the shifted factor. Provided that C_{i+k} is known, we can easily recover Ψ_{i+k} from $\widetilde{\Psi}_{i+k}$. Therefore, leaving the original condition (20) aside, we will consider how to satisfy the following condition, i.e.,

$$\mathrm{abs}(\widetilde{\Psi}_{i+k}) \leq \pi/2. \tag{26}$$

To satisfy the above inequality (26), we should select a suitable C_{i+k} such that $\widetilde{\Psi}_{i+k}$ is symmetrically distributed. In such an approach, the maximal absolute of $\widetilde{\Psi}_{i+k}$ is minimized, and then condition (26) can be satisfied more easily. Moreover, one recalls (23) and gets that

$$(\phi_i + \phi_k)/2 \in [-\Delta, \Delta] \tag{27}$$

which implies that $(\phi_i + \phi_k)/2$ is symmetrically distributed. Since $\widetilde{\Psi}_{i+k} = \pi\lambda^{-1}(\mathbf{p}_i + \mathbf{p}_k)^{\mathrm{T}}\mathbf{r} + (\phi_i + \phi_k)/2 - C_{i+k}$, the above discussion suggests that a (good) sufficient condition satisfying (26) is given by

$$\pi\lambda^{-1}(\mathbf{p}_i + \mathbf{p}_k)^{\mathrm{T}}\mathbf{r} - C_{i+k} \in [-\Delta_{i+k}, \Delta_{i+k}], \ \forall\theta \in \mathcal{D} \tag{28a}$$

$$\Delta + \Delta_{i+k} \leq \pi/2. \tag{28b}$$

Note that in (28a), a dummy variable Δ_{i+k} is introduced so that the resultant $\pi\lambda^{-1}(\mathbf{p}_i + \mathbf{p}_k)^{\mathrm{T}}\mathbf{r} - C_{i+k}$ is symmetrically distributed.

To satisfy condition (28a), we can set C_{i+k} as

$$C_{i+k} = \left(\alpha_{\max}^{(i+k)} + \alpha_{\min}^{(i+k)}\right)/2 \tag{29}$$

with $\alpha_{\max}^{(i+k)}$ and $\alpha_{\min}^{(i+k)}$ being determined by

$$\alpha_{\max}^{(i+k)} = \max_{\theta\in\mathcal{D}} \left(\pi\lambda^{-1}(\mathbf{p}_i + \mathbf{p}_k)^{\mathrm{T}}\mathbf{r}\right) \tag{30a}$$

$$\alpha_{\min}^{(i+k)} = \min_{\theta\in\mathcal{D}} \left(\pi\lambda^{-1}(\mathbf{p}_i + \mathbf{p}_k)^{\mathrm{T}}\mathbf{r}\right). \tag{30b}$$

Under the above settings of (29) and (30), it yields

$$\Delta_{i+k} = \left(\alpha_{\max}^{(i+k)} - \alpha_{\min}^{(i+k)}\right)/2. \tag{31}$$

Furthermore, combining (28) and (31), the sufficient condition to satisfy (26) can be expressed as

$$\Delta + \left(\alpha_{\max}^{(i+k)} - \alpha_{\min}^{(i+k)}\right)/2 \leq \pi/2. \tag{32}$$

Consequently, (26) becomes true once the above inequality (32) has been satisfied. It should be also noted that for a given pair of i and k, one can determine whether formula (32) is valid offline, i.e., not relying on the snapshot data $\mathbf{X}$. What remains may be how to further obtain an estimate of $\widetilde{\Psi}_{i+k}$ and then build a linear equation with respect to the unknown θ and ϕ_n. We will present the details next.

Generally speaking, $\widetilde{\Psi}_{i+k}$ can be similarly obtained with the procedure described in the previous section, except for carrying out a compensation $e^{-jC_{i+k}}$ for data $\mathbf{X}$.

More specifically, if (32) is satisfied for the given pair i and k, we can utilize $e^{-jC_{i+k}}$ to compensate $\mathbf{X}(i,:)$ and $\mathbf{X}(k,:)$, and then sum them up to obtain $\widetilde{\mathbf{X}}_{i+k}$ as

$$\widetilde{\mathbf{X}}_{i+k} = \mathbf{X}(i,:)e^{-jC_{i+k}} + \mathbf{X}(k,:)e^{-jC_{i+k}}. \tag{33}$$

Recalling (11), $\widetilde{\mathbf{X}}_{i+k}$ can be further expressed as

$$\widetilde{\mathbf{X}}_{i+k} = c_{i+k}e^{j\widetilde{\Psi}_{i+k}}\mathbf{S} + \widetilde{\mathbf{N}}_{i+k} \tag{34}$$

where $\widetilde{\mathbf{N}}_{i+k} = \mathbf{N}(i,:)e^{-jC_{i+k}} + \mathbf{N}(k,:)e^{-jC_{i+k}}$. Notice that the item $\widetilde{\Psi}_{i+k} = \Psi_{i+k} - C_{i+k}$ has appeared in (34). Since $\mathrm{abs}(\widetilde{\Psi}_{i+k}) \leq \pi/2$, an estimation of $\widetilde{\Psi}_{i+k}$ can be unambiguously obtained as

$$\widetilde{\Psi}_{i+k} = \angle(\widetilde{\boldsymbol{\gamma}}_{i+k}(2)) \tag{35}$$

where $\widetilde{\boldsymbol{\gamma}}_{i+k}$ is the principal left singular vector of $\widetilde{\mathbf{Y}}_{i+k}$ satisfying

$$\widetilde{\mathbf{Y}}_{i+k} = \begin{bmatrix} \mathbf{X}(1,:) \\ \widetilde{\mathbf{X}}_{i+k} \end{bmatrix} = \begin{bmatrix} 1 & \\ & e^{-jC_{i+k}} \end{bmatrix} \mathbf{Y}_{i+k} \tag{36}$$

with $\mathbf{Y}_{i+k}$ being defined as in (16). Note that in (35), we implicitly assumed that $\widetilde{\boldsymbol{\gamma}}_{i+k}$ is the normalized version with a unit in its first entry.

Once $\widetilde{\Psi}_{i+k}$ has been estimated, we can construct the following linear equation:

$$\mathbf{w}_{i+k}^{\mathrm{T}}\mathbf{v} = \angle[\widetilde{\boldsymbol{\gamma}}_{i+k}(2)] - \phi_c\mathbf{b}(c) + C_{i+k} \triangleq d_{i+k}. \tag{37}$$

Here, note that we establish the above equation on the basis of $\widetilde{\boldsymbol{\gamma}}_{i+k}$, not using $\boldsymbol{\gamma}_{i+k}$. Since condition (32) is more easily satisfied than (20), we can say that more equations like (37) can be obtained. As a consequence, the practicality of the proposed scheme is greatly improved.

C. LSs Problem With a Quadratic Constraint

Given i and k, a practical strategy is provided in the previous section to construct a linear equation [i.e., (37)] with respect to the unknown DOA θ and phase error ϕ, under specific condition. As pointed out in Section III-A, one can build a certain number (up to $N(N-1)/2$ at most) of linear equations by taking different values of i and k, with $i, k = 1, 2, \ldots, N$ and $i \neq k$. By doing so, all the unknown parameters may be well recovered.

More specifically, let us define $\mathbf{W}$ as the matrix piled up by $\mathbf{w}_{i+k}^{\mathrm{T}}$ along column direction, and define $\mathbf{d}$ as the data vector piled up by d_{i+k}, where i and k are some specific indexes that satisfy (32). Then, the problem of DOA and phase error estimation can be described as the following LS optimization problem with a quadratic constraint:

$$\min_{\mathbf{v}} \ \|\mathbf{W}\mathbf{v}-\mathbf{d}\|_2^2 \tag{38a}$$

$$\text{s.t. } \|\mathbf{Z}\mathbf{v}\|_2^2 = 1 \tag{38b}$$

where the constraint matrix $\mathbf{Z} = \left[\mathbf{O}_{2\times(N-2)}\ \mathbf{I}_2\right]$ is introduced to satisfy $\cos^2\theta+\sin^2\theta = 1$, and $\|\cdot\|_2$ stands for the Euclidean norm. It is known from [42] that the problem of (38) can be solved provided that

$$\text{rank}\left(\left[\mathbf{W}^{\mathrm{T}}\ \mathbf{Z}^{\mathrm{T}}\right]^{\mathrm{T}}\right) = N \tag{39}$$

which can be determined offline without using any snapshot data. Once problem (38) has been solved (denote the solution as $\widehat{\mathbf{v}}$), the DOA θ and phase error ϕ can be estimated out accordingly. More precisely, the unknown θ and ϕ can be obtained as

$$\widehat{\theta} = \text{asin}(\widehat{\mathbf{v}}(N)) \tag{40}$$

and

$$\widehat{\phi}_n = \begin{cases} \widehat{\mathbf{v}}(n-1), \text{ if } 2 \le n < c \\ \widehat{\mathbf{v}}(n-2), \text{ if } c < n \le N \end{cases} \tag{41}$$

respectively. Clearly, one problem remained is how to solve the optimization problem (38). We will take this issue into consideration in the following section.

REMARK 2 Note that formulation (38) is developed on the basis of a general 2-D array. For the 1-D linear array, constraint (38b) becomes unnecessary and a traditional LS problem can be resulted. In this case, we can obtain DOA and phase errors with a closed-form expression.

D. Approach to Solving Problem (38)

In our previous work [1], we have presented two solvers, i.e., GSVD and SDR, to find the solution of the nonconvex problem (38). For the GSVD-based method, it needs to solve a nonlinear equation that may be computationally inefficient. As for the second solver, i.e., the SDR-based method, it may bring a performance loss since the original problem is relaxed for computation convenience. To overcome these imperfections, in this section we use the CCP to solve problem (38). As shown in our later simulations, the CCP approach obtains a better performance than that of the SDR method.

Basically, CCP is a powerful method used to find solutions to difference of convex (DC) programming problems. As pointed out in [40], the class of DC functions is very broad, and a DC program is not convex so that it is hard to solve in general. In CCP approach, the original DC program is solved by iteratively conducting convexifying procedure and solving the convex program. As shown in [40], the convergence property of CCP can be well guaranteed.

To apply the CCP approach, we first reformulate problem (38) as

$$\min_{\mathbf{v}} \ \mathbf{v}^{\mathrm{T}}\mathbf{W}^{\mathrm{T}}\mathbf{W}\mathbf{v} - 2\mathbf{d}^{\mathrm{T}}\mathbf{W}\mathbf{v} \tag{42a}$$

$$\text{s.t. } \mathbf{v}^{\mathrm{T}}\mathbf{Z}^{\mathrm{T}}\mathbf{Z}\mathbf{v} = 1. \tag{42b}$$

By carrying out the eigenvalue decomposition procedure, one obtains that

$$\begin{aligned}\mathbf{W}^{\mathrm{T}}\mathbf{W} &= \sum_{n=1}^{N}\lambda_n\mathbf{q}_n\mathbf{q}_n^{\mathrm{H}} \\ &= \underbrace{\sum_{n=1}^{C}\lambda_n\mathbf{q}_n\mathbf{q}_n^{\mathrm{H}}}_{\triangleq\mathbf{B}_+} - \underbrace{\sum_{n=C+1}^{N}|\lambda_n|\mathbf{q}_n\mathbf{q}_n^{\mathrm{H}}}_{\triangleq\mathbf{B}_-}\end{aligned} \tag{43}$$

where λ_n and $\mathbf{q}_n$ $(n = 1, \ldots, N)$ denote the eigenvalue and its corresponding eigenvector, respectively. Moreover, it is assumed that the eigenvalues have been arranged to satisfy

$$\lambda_1 \ge \cdots \ge \lambda_C \ge 0 > \lambda_{C+1}\cdots \ge \lambda_N. \tag{44}$$

According to (44), it is easily found that the matrices $\mathbf{B}_+$ and $\mathbf{B}_-$ in (43) are positive semidefinite.

On the other hand, one also readily derives that

$$\begin{aligned}\mathbf{Z}^{\mathrm{T}}\mathbf{Z} &= \begin{bmatrix}\mathbf{O_{N-2}} & \mathbf{O}_{(N-2)\times 2} \\ \mathbf{O}_{2\times(N-2)} & \mathbf{I}_2\end{bmatrix} \\ &= \underbrace{\mathbf{I}_N}_{\triangleq\mathbf{P}_+} - \underbrace{\begin{bmatrix}\mathbf{I_{N-2}} & \mathbf{O}_{(N-2)\times 2} \\ \mathbf{O}_{2\times(N-2)} & \mathbf{O}_2\end{bmatrix}}_{\triangleq\mathbf{P}_-}.\end{aligned} \tag{45}$$

Obviously, both $\mathbf{P}_+$ and $\mathbf{P}_-$ above are positive semidefinite.

As a consequence, problem (42) is equivalent to

$$\min_{\mathbf{v}} \ \mathbf{v}^{\mathrm{T}}\mathbf{B}_+\mathbf{v} - (\mathbf{v}^{\mathrm{T}}\mathbf{B}_-\mathbf{v} + 2\mathbf{d}^{\mathrm{T}}\mathbf{W}\mathbf{v}) \tag{46a}$$

$$\text{s.t. } \mathbf{v}^{\mathrm{T}}\mathbf{P}_+\mathbf{v} - \mathbf{v}^{\mathrm{T}}\mathbf{P}_-\mathbf{v} = 1 \tag{46b}$$

where $\mathbf{B}_+$, $\mathbf{B}_-$, $\mathbf{P}_+$, and $\mathbf{P}_-$ have been defined in (43) and (45). Apparently, the objective function in (46a) is a DC one. Therefore, the CCP approach can be employed as long as constraint (46b) is also a DC function. To this end, we further reformulate problem (46) as

$$\min_{\mathbf{v}} \ \underbrace{\mathbf{v}^{\mathrm{T}}\mathbf{B}_+\mathbf{v}}_{\triangleq f_0(\mathbf{v})} - \underbrace{(\mathbf{v}^{\mathrm{T}}\mathbf{B}_-\mathbf{v} + 2\mathbf{d}^{\mathrm{T}}\mathbf{W}\mathbf{v})}_{\triangleq h_0(\mathbf{v})} \tag{47a}$$

$$\text{s.t. } \underbrace{\mathbf{v}^{\mathrm{T}}\mathbf{P}_+\mathbf{v}}_{\triangleq f_1(\mathbf{v})} - \underbrace{(\mathbf{v}^{\mathrm{T}}\mathbf{P}_-\mathbf{v}+1)}_{\triangleq h_1(\mathbf{v})} \le 0 \tag{47b}$$

$$\underbrace{(\mathbf{v}^{\mathrm{T}}\mathbf{P}_-\mathbf{v}+1)}_{\triangleq f_2(\mathbf{v})} - \underbrace{\mathbf{v}^{\mathrm{T}}\mathbf{P}_+\mathbf{v}}_{\triangleq h_2(\mathbf{v})} \le 0. \tag{47c}$$

It can be seen that all the functions $f_l(\mathbf{v})$ and $h_l(\mathbf{v})$ $(l = 0, 1, 2)$ in problem (47) are convex, due to the fact that $\mathbf{B}_+$, $\mathbf{B}_-$, $\mathbf{P}_+$, and $\mathbf{P}_-$ are positive semidefinite. Then according to the definition in [40], problem (47) is a DC program, which can be solved by CCP approach.

In CCP method, more specifically, the procedure is started from an initial point in the feasible set. For problem (42) or (47), we can set $k = 1$ and initialize

$$\mathbf{v}_1 = [0, \ldots, 0, \cos(\theta_0), \sin(\theta_0)]^{\mathrm{T}} \in \mathbb{R}^N \tag{48}$$

Algorithm 1: CCP Approach to Solving Problem (38).

set $k = 1$ and initialize $\mathbf{v}_1$ by (48)
while not convergent **do**
  solve problem (51) and denote the solution as $\mathbf{v}_{k,\star}$
  set $k = k + 1$
  set $\mathbf{v}_k = \mathbf{v}_{k-1,\star}$
end while
output the solution $\widehat{\mathbf{v}} = \mathbf{v}_k$

Algorithm 2: Proposed Algorithm.

give a coarse estimation of θ and set the result as θ_0, denote the perturbation of DOA estimation by δ, prescribe the maximum value of $|\phi_n|$ $(n = 1, 2, \cdots, N)$ as Δ.
for $i = 1 \to N$ **do**
  for $k = 1 \to N, k \neq i$ **do**
    obtain $\alpha_{\max}^{(i+k)}$ and $\alpha_{\min}^{(i+k)}$ by (30)
    if condition (32) is true **then**
      obtain vector $\mathbf{b}_{i+k}$ from (15)
      obtain vector $\mathbf{w}_{i+k}$ by modifying $\mathbf{b}_{i+k}$
      compute C_{i+k} using (29)
      obtain $\widetilde{\mathbf{X}}_{i+k}$ as (33)
      construct $\widetilde{\mathbf{Y}}_{i+k}$ as (36)
      compute $\widetilde{\boldsymbol{\gamma}}_{i+k}$ through SVD of $\widetilde{\mathbf{Y}}_{i+k}$
      obtain d_{i+k} from (37)
    end if
  end for
end for
construct $\mathbf{W}$ and $\mathbf{d}$
if rank $\left(\left[\mathbf{W}^{\mathrm{T}}\ \mathbf{Z}^{\mathrm{T}}\right]^{\mathrm{T}}\right) == N$ **then**
  solve problem (38) by using the CCP approach (see Algorithm 1) and obtain the solution $\widehat{\mathbf{v}}$
  obtain $\widehat{\theta}$ and $\widehat{\phi}_n$ from (40) and (41), respectively
else
  set $\widehat{\theta} = \theta_0$ and $\widehat{\phi}_n = 0$ $(n = 2, \ldots, c-1, c+1, \ldots, N)$
end if
Output: $\widehat{\theta}$ and $\widehat{\phi}_n$.

where θ_0 is a coarse estimation of the DOA as we aforementioned. In the kth step of the CCP approach, problem (47) is convexified by replacing $h_l(\mathbf{v})$ $(l = 0, 1, 2)$ with the function $\hat{h}_l(\mathbf{v}; \mathbf{v}_k)$ as

$$\hat{h}_l(\mathbf{v}; \mathbf{v}_k) \triangleq h_l(\mathbf{v}_k) + \bigtriangledown h_l^{\mathrm{T}}(\mathbf{v}_k)(\mathbf{v} - \mathbf{v}_k),\ l = 0, 1, 2. \tag{49}$$

Since $\hat{h}_l(\mathbf{v}; \mathbf{v}_k)$ is affine with respect to $\mathbf{v}$, we know that $f_l(\mathbf{v}) - \hat{h}_l(\mathbf{v}; \mathbf{v}_k)$ is convex for $l = 0, 1, 2$. More precisely, we have

$$\begin{aligned} \hat{h}_0(\mathbf{v}; \mathbf{v}_k) &= h_0(\mathbf{v}_k) + 2(\mathbf{v}_k^{\mathrm{T}}\mathbf{B}_- + \mathbf{d}^{\mathrm{T}}\mathbf{W})(\mathbf{v} - \mathbf{v}_k) \\ &= 2(\mathbf{v}_k^{\mathrm{T}}\mathbf{B}_- + \mathbf{d}^{\mathrm{T}}\mathbf{W})\mathbf{v} - \mathbf{v}_k^{\mathrm{T}}\mathbf{B}_-\mathbf{v}_k \end{aligned} \tag{50a}$$

$$\begin{aligned} \hat{h}_1(\mathbf{v}; \mathbf{v}_k) &= h_1(\mathbf{v}_k) + 2\mathbf{v}_k^{\mathrm{T}}\mathbf{P}_-(\mathbf{v} - \mathbf{v}_k) \\ &= 2\mathbf{v}_k^{\mathrm{T}}\mathbf{P}_-\mathbf{v} - \mathbf{v}_k^{\mathrm{T}}\mathbf{P}_-\mathbf{v}_k + 1 \end{aligned} \tag{50b}$$

$$\begin{aligned} \hat{h}_2(\mathbf{v}; \mathbf{v}_k) &= h_2(\mathbf{v}_k) + 2\mathbf{v}_k^{\mathrm{T}}\mathbf{P}_+(\mathbf{v} - \mathbf{v}_k) \\ &= 2\mathbf{v}_k^{\mathrm{T}}\mathbf{P}_+\mathbf{v} - \mathbf{v}_k^{\mathrm{T}}\mathbf{P}_+\mathbf{v}_k. \end{aligned} \tag{50c}$$

Accordingly, the convexified version of (47) (by replacing $h_l(\mathbf{v})$ with $\hat{h}_l(\mathbf{v}; \mathbf{v}_k)$, $l = 0, 1, 2$) becomes

$$\min_{\mathbf{v}}\ \mathbf{v}^{\mathrm{T}}\mathbf{B}_+\mathbf{v} - 2(\mathbf{v}_k^{\mathrm{T}}\mathbf{B}_- + \mathbf{d}^{\mathrm{T}}\mathbf{W})\mathbf{v} \tag{51a}$$

$$\text{s.t. } \mathbf{v}^{\mathrm{T}}\mathbf{P}_+\mathbf{v} \leq 2\mathbf{v}_k^{\mathrm{T}}\mathbf{P}_-\mathbf{v} - \mathbf{v}_k^{\mathrm{T}}\mathbf{P}_-\mathbf{v}_k + 1 \tag{51b}$$

$$\mathbf{v}^{\mathrm{T}}\mathbf{P}_-\mathbf{v} + 1 \leq 2\mathbf{v}_k^{\mathrm{T}}\mathbf{P}_+\mathbf{v} - \mathbf{v}_k^{\mathrm{T}}\mathbf{P}_+\mathbf{v}_k. \tag{51c}$$

Once the solution to (51) (denoted as $\mathbf{v}_{k,\star}$) has been obtained, we can set $k = k + 1$, and then resolve problem (51) by taking $\mathbf{v}_k = \mathbf{v}_{k-1,\star}$. This procedure is repeatedly carried out until a convergence criterion is satisfied. Finally, we can obtain the estimation of $\mathbf{v}$ as $\widehat{\mathbf{v}} = \mathbf{v}_k$. This completes the solving of problem (38). To make it clear, we summarize the CCP approach to problem (38) in Algorithm 1.

As aforementioned, once the solution $\widehat{\mathbf{v}}$ to problem (38) has been obtained, the DOA and phase error can be uniquely determined. To conclude, we give a step-by-step description of the proposed approach in Algorithm 2.

REMARK 3 Note that in the above discussions, we assume that one sensor has been calibrated. This condition can be satisfied in some cases as mentioned in [33]–[39]. For an existing array that is completely uncalibrated, our algorithm still works if we first select a sensor as the calibrated one. More specifically, in this case we can first apply the self-calibration algorithm (e.g., methods in [29] and [30] for ULAs and methods in [20] and [26] for arbitrary arrays) to obtain a rough estimation of DOA and phase error. Then, the sensor (excluding the reference one) with the less phase error estimation deviation (from the presumed value) is selected as the calibrated sensor for our method (mainly because it is more likely to obtain a relatively high estimation accuracy), and the corresponding estimated phase error is set as the calibrated value (i.e., ϕ_c in the above discussions). Finally, we can carry out our algorithm to obtain a better estimation using the automatically specified calibrated sensor. Numerical test shows that this strategy works well as presented in the simulation part. Moreover, the above scheme makes the proposed method feasible to calibrate arrays without any additional assumptions, by simply assigning a calibration source with inaccurate orientation. Also, with the above procedures, we can automatically calibrate multiple antenna arrays with the same kind, by applying the above-mentioned approach to one sampling of the arrays. This is extremely practical when antenna arrays are available on chips.

IV. CRAMÉR–RAO BOUNDS

In this section, we give the CRBs for the estimations of DOA and phase error in the original problem statement in Section II.

From Section II, one can readily express the covariance matrix as

$$\mathbf{R} = \sigma_s^2 \Gamma \mathbf{a}(\theta)\mathbf{a}^{\mathrm{H}}(\theta)\Gamma^{\mathrm{H}} + \sigma_n^2 \mathbf{I} = \sigma_s^2 \mathbf{a}_r(\theta)\mathbf{a}_r^{\mathrm{H}}(\theta) + \sigma_n^2 \mathbf{I}.$$

Following the derivation result in [37], the CRB for the unknown DOA θ can be given by

$$\mathrm{CRB}(\theta) = \frac{1}{2\sigma_s^4 N}\Big\{\Re\Big(\mathbf{a}_r^{\mathrm{H}}(\theta)\mathbf{R}^{-1}\mathbf{a}_r(\theta)\dot{\mathbf{a}}_r^{\mathrm{H}}(\theta)\mathbf{R}^{-1}\dot{\mathbf{a}}_r(\theta) + \big(\mathbf{a}_r^{\mathrm{H}}(\theta)\mathbf{R}^{-1}\dot{\mathbf{a}}_r(\theta)\big)^2\Big)\Big\}^{-1}$$

where $\dot{\mathbf{a}}_r(\theta)$ is defined as

$$\dot{\mathbf{a}}_r(\theta) \triangleq \frac{\partial \mathbf{a}_r(\theta)}{\partial \theta}. \tag{52}$$

On the other hand, denote

$$\boldsymbol{\phi} = [\phi_2, \ldots, \phi_{c-1}, \phi_{c+1}, \ldots, \phi_N]^{\mathrm{T}}. \tag{53}$$

Then, the CRB for the phase error estimation can be obtained according to [37] as

$$\mathrm{CRB}(\boldsymbol{\phi}) = \frac{1}{2\sigma_s^4 N}\Big\{\Re\Big(\mathbf{J}\big[\big(\mathbf{a}_r(\theta)\mathbf{a}_r^{\mathrm{H}}(\theta)\mathbf{R}^{-1}\mathbf{a}_r(\theta)\mathbf{a}_r^{\mathrm{H}}(\theta)\big) \odot (\mathbf{R}^{-1})^{\mathrm{T}} - \big(\mathbf{a}_r(\theta)\mathbf{a}_r^{\mathrm{H}}(\theta)\mathbf{R}^{-1}\big) \odot \big(\mathbf{a}_r(\theta)\mathbf{a}_r^{\mathrm{H}}(\theta)\mathbf{R}^{-1}\big)^{\mathrm{T}}\big]\mathbf{J}^{\mathrm{T}}\Big)\Big\}^{-1}$$

where $\mathbf{J}$ is an $(N-2) \times N$ matrix with its (i, j)th entry being

$$\mathbf{J}_{i,j} = \begin{cases} 1, & \text{if } i \leq c-2 \text{ and } i = j-1 \\ 1, & \text{if } i > c-2 \text{ and } i = j-2 \\ 0, & \text{otherwise} \end{cases}. \tag{54}$$

We will use $\mathrm{CRB}(\theta)$ and $\mathrm{CRB}(\boldsymbol{\phi})$ to measure the performance of DOA and phase error estimation in the following section.

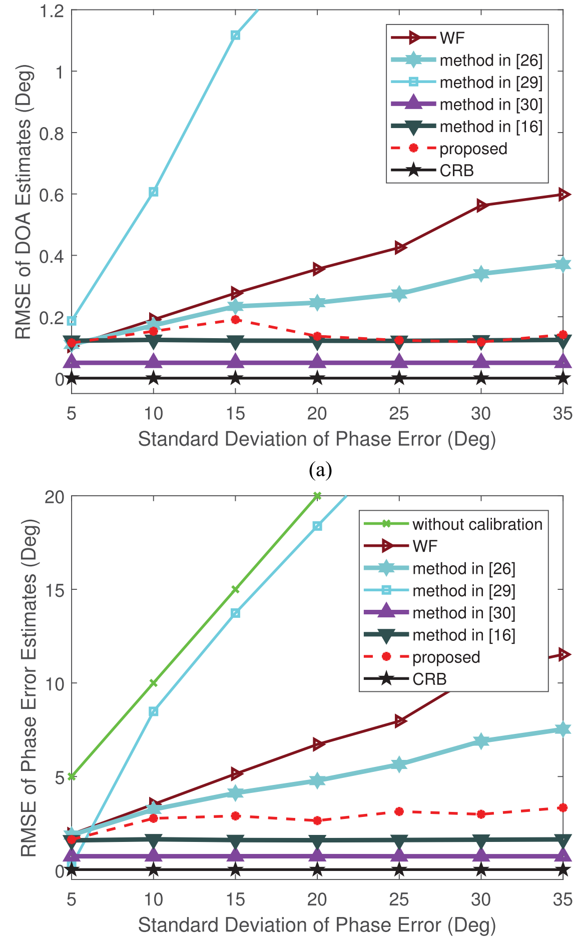

Fig. 3. RMSEs of estimates versus standard deviation of phase error for a ULA. (a) DOA estimation. (b) Phase error estimation.

V. NUMERICAL RESULTS

In this section, representative simulations are carried out to demonstrate the effectiveness of the proposed method. The phase error $\{\phi_n\}_{n=1}^N$ of sensors is generated by [21]

$$\phi_n = \sqrt{12}\sigma_\phi \beta_n \tag{55}$$

where β_n is independent and identically distributed random variable, which is distributed uniformly in the range of $[-0.5, 0.5]$, σ_ϕ acts as the standard deviation of ϕ_n, $n = 1, \ldots, N$. To present the performance of the proposed method, we next consider three cases using two arrays with different geometries. Note that in the former two cases the array contains a calibrated sensor, whereas in the third case we use a fully uncalibrated array as an extension to show the wide applicability of the proposed algorithm.

A. ULA With One Calibrated Sensor

In the first case, let us consider a ULA of $N = 15$ elements spaced by half wavelength. The elements are labeled in sequence from 1 to N. The first sensor is assumed to have been calibrated (i.e., $c = 1$) and the eighth sensor (locating at origin) is taken as the reference one. Consider one signal impinging on the array. The direction of signal is $\theta = 12.9^\circ$, and we know *a priori* that θ is in the range $[\theta_0 - \delta_\theta, \theta_0 + \delta_\theta]$ with $\theta_0 = 9^\circ$ and $\delta_\theta = 8^\circ$. In addition, we set $\mathrm{SNR} = 15$ dB and $L = 500$, and measure the root-mean-square error (RMSE) of DOA and phase error estimates versus the standard deviation of phase error (i.e., σ_ϕ). For comparison purpose, the WF method in [20], the subspace method in [26], the array interpolation method in [16], and the eigenstructure methods in [29] and [30] will be carried out and then compared with the proposed one, and the CRBs will also be considered as a benchmark. As aforementioned in Remark 2, in this case, our method provides a closed-form solution to the unknown DOA and phase error.

The resulting curves are presented in Fig. 3, from which one can clearly see that the proposed method performs better than the WF method, the subspace method in [26], and the eigenstructure method in [29]. Moreover, Fig. 3 shows that the performance of our approach is nearly independent of the standard deviation of phase error. In addition, we can see that the resulting RMSEs of the array interpolation method in [16] and the eigenstructure method in [30] are close to the CRBs and lower than those of the proposed

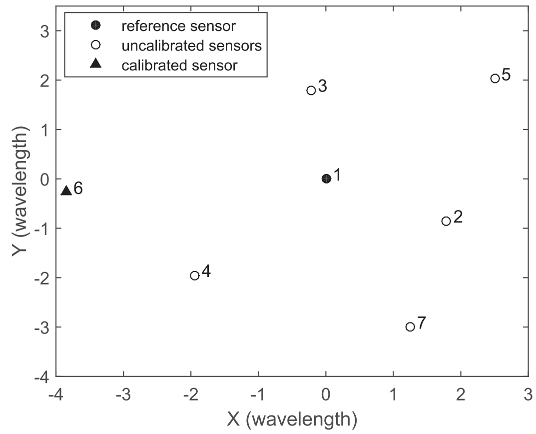

Fig. 4. Array configuration.

TABLE I
Element Positions of a Planar Array

n	$x_n(\lambda)$	$y_n(\lambda)$	n	$x_n(\lambda)$	$y_n(\lambda)$
1	0.00	0.00	5	2.50	2.03
2	1.79	-0.85	6	-3.84	-0.27
3	-0.22	1.80	7	1.25	-3.00
4	-1.94	-1.95			

one. Nevertheless, the method in [16] requires several calibration sources with known directions, which is difficult to deploy in practical engineering. For the approach in [30], it is only suitable for ULAs and cannot be applied to arrays with other geometries as shown in the following.

B. 2-D Planar Array With One Calibrated Sensor

To show that the proposed method is applicable to an array with arbitrary geometry, we now consider a planar array with $N = 7$ omnidirectional sensors, as shown in Fig. 4. The element locations are specified in Table I. More specifically, the first element that locates at origin is taken as the reference one, and the sixth (i.e., $c = 6$) element has been calibrated. Considering one signal that impinges on the array from $\theta = 26^\circ$, we have known that the real DOA is located in the range $[\theta_0 - \delta_\theta, \theta_0 + \delta_\theta]$ with $\theta_0 = 24^\circ$ and $\delta_\theta = 8^\circ$. Unless otherwise specified, we set $\sigma_\phi = 10^\circ$, SNR = 15 dB, and $L = 400$. In this case, a constrained LS problem [see (38)] can be formulated in our method, and the CCP approach will be used to find the ultimate solution. In addition, the WF method in [20], the subspace method in [26], the array interpolation method in [16], and the two optimization approaches (i.e., GSVD and SDR) in [1] will also be carried out for comparison.

Before presenting the performance of DOA and phase error estimation, we first test the convergence of the CCP approach. To do so, we follow the analysis in Section III-D and define

$$J_k \triangleq \mathbf{v}_k^{\mathrm{T}} \mathbf{B}_+ \mathbf{v}_k - 2(\mathbf{v}_k^{\mathrm{T}} \mathbf{B}_- + \mathbf{d}^{\mathrm{T}} \mathbf{W}) \mathbf{v}_k \tag{56}$$

$$\Delta_k \triangleq J_k - J_{k+1}. \tag{57}$$

Clearly, J_k is the resulting cost value of problem (51) after carrying out the kth step of CCP process. Δ_k denotes the cost difference of the kth iteration and the $(k+1)$th iteration, and is expected to be small enough if CCP converges. Following the parameter setting in Table II, we carry out the CCP approach in Algorithm 1 and depict the resulting curves of J_k and Δ_k versus the iteration step k in Figs. 5 and 6, respectively. As expected, the cost value J_k monotone decreases with iteration. Moreover, one can see that Δ_k becomes lower than 10^{-4} and stays nearly unchanged after carrying out the third iteration step. This shows that the CCP approach converges with only a few iteration steps. In fact, the behavior of Δ_k is similar to those of the estimation accuracies of DOA and phase errors. To see this point clear, we denote by $D_k(\theta)$ and $D_k(\phi)$ the estimation deviation of DOA and the average estimation deviation of phase errors at the kth iteration step, respectively. The curves of $D_k(\theta)$ and $D_k(\phi)$ versus the iteration step are depicted in Figs. 7 and 8, respectively. One can see that both $D_k(\theta)$ and $D_k(\phi)$ decrease with iteration before convergence. The resulting

TABLE II
Parameter Comparison of One Realization of Our Method

	ϕ_2	ϕ_3	ϕ_4	ϕ_5	ϕ_7	θ
real	13.217°	1.247°	-11.619°	10.147°	6.170°	26.000°
estimated	14.227°	0.160°	-10.953°	8.957°	8.934°	25.993°

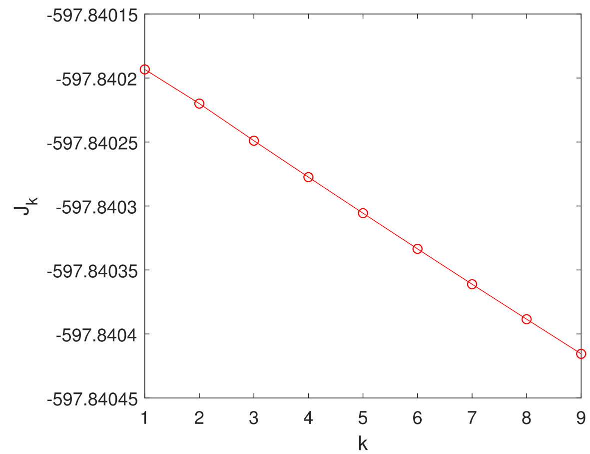

Fig. 5. Curve of J_k versus the iteration step.

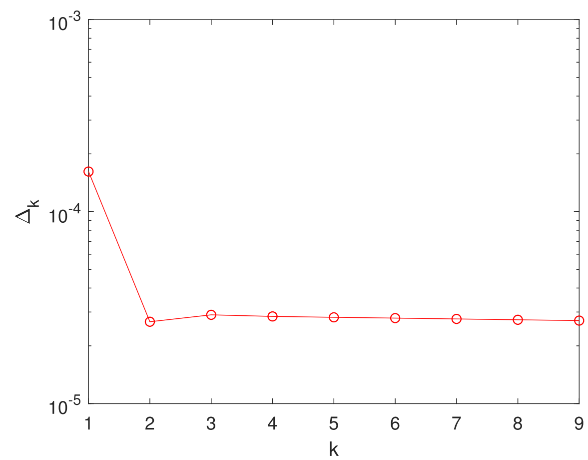

Fig. 6. Curve of Δ_k versus the iteration step.

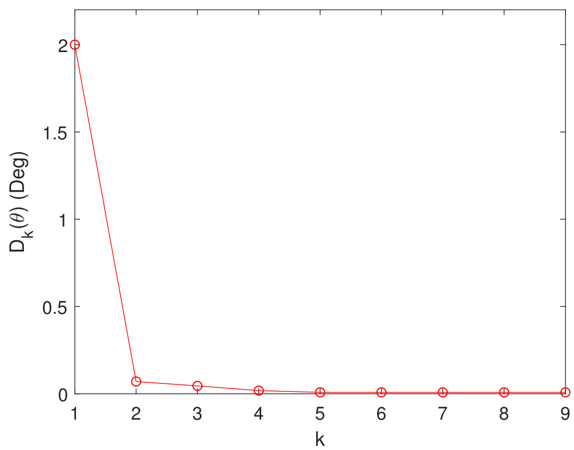

Fig. 7. Curve of $D_k(\theta)$ versus the iteration step.

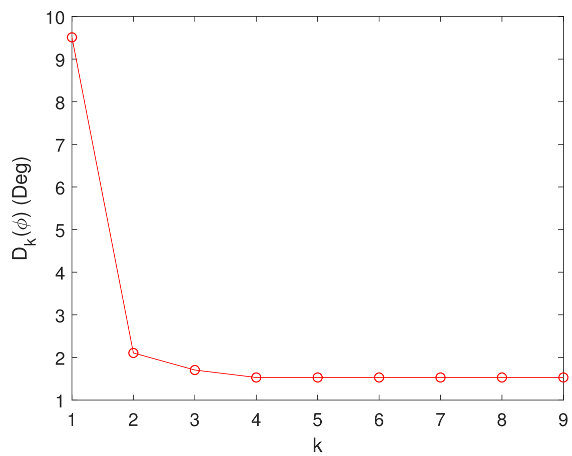

Fig. 8. Curve of $D_k(\phi)$ versus the iteration step.

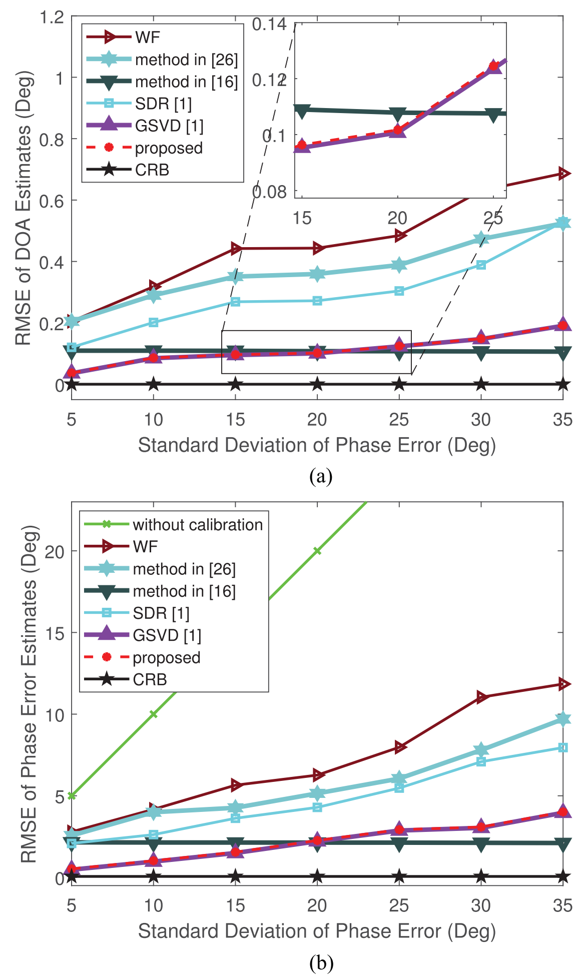

Fig. 9. RMSEs of estimates versus standard deviation of phase error. (a) DOA estimation. (b) Phase error estimation.

estimations of DOA and phase errors have been listed in Table II. We can see that the estimated values are close to the real ones. The GSVD approach in [1] obtains similar results in this realization. For the SDR approach in [1], a good performance may not be always guaranteed, as we presented more specifically in the following.

1) *Estimation Performance Versus the Standard Deviation of Phase Error:* In this part, the performance in terms of the RMSEs versus the standard deviation of phase error (i.e., σ_ϕ) is studied. We vary σ_ϕ from 5° to 35° and depict the RMSEs of different methods in Fig. 9. It can be seen that the WF method, the subspace method in [26], and the SDR approach in [1] perform worse than those of our method and the GSVD approach in [1]. Although the array interpolation method in [16] performs better than the proposed one especially when σ_ϕ is greater than 25°, it requires additional sources with known directions to complete the calibration. Observe from Fig. 9 that the curves of our CCP method and the GSVD method are almost identical. In fact, the GSVD algorithm performs slightly better than the proposed algorithm for the current simulation settings. This is because that the performance of our method may be somewhat affected by the iteration number and/or termination criterion. Meanwhile, we can see that all the methods tested degrade as σ_ϕ increases. For our method, the possible reason of this behavior may be that the larger σ_ϕ is, the less number of equations (37) can be developed, and then the resulting performance may degrade. In addition, it should be pointed out that the size of variable in the LS problem also influences the ultimate accuracy. Nevertheless, we should emphasize that the above behavior is not universal applicable (see Fig. 3 for counterexample), and the performance trend (as σ_ϕ increases) of the proposed method depends upon circumstances.

2) *Estimation Performance Versus SNR:* We now test the estimation performance of the proposed method under different SNR settings. Fig. 10 illustrates the resulting curves of RMSEs. It can be seen that the proposed method performs better than the WF method, the subspace method in [26], and the SDR approach in [1]. Moreover, the superiority of the proposed method becomes more obvious in the high SNR scenario, and our algorithm outperforms the array interpolation method in [16] when SNR is greater than 10 dB. In addition, the proposed CCP-based method performs almost the same as the GSVD method, although the latter shows negligible improvements after zooming in the results.

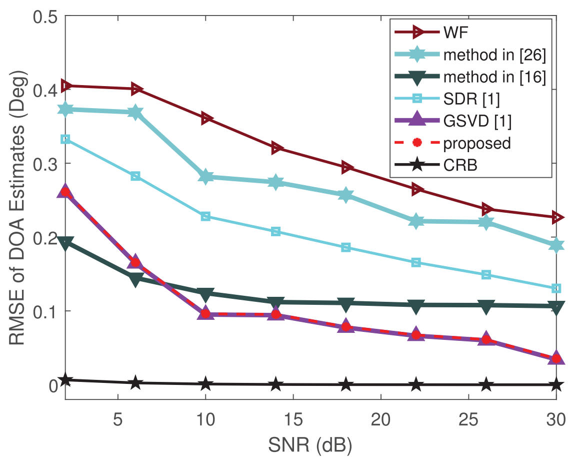

(a)

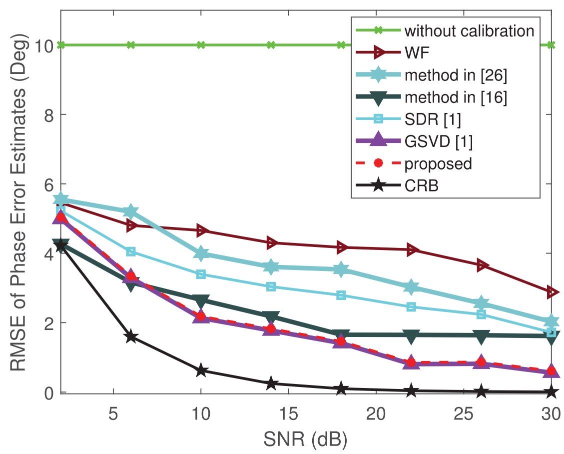

(b)

Fig. 10. RMSEs of estimates versus SNR. (a) DOA estimation. (b) Phase error estimation.

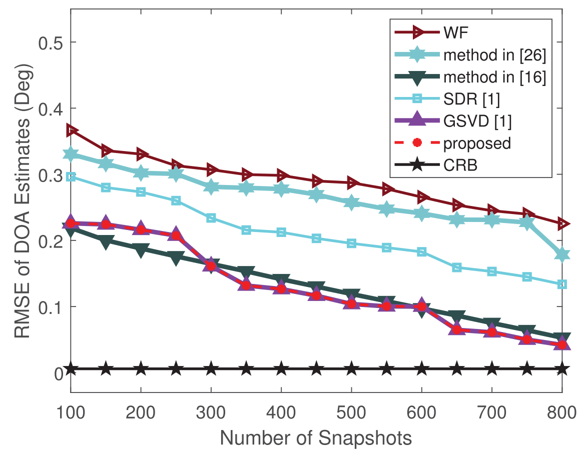

(a)

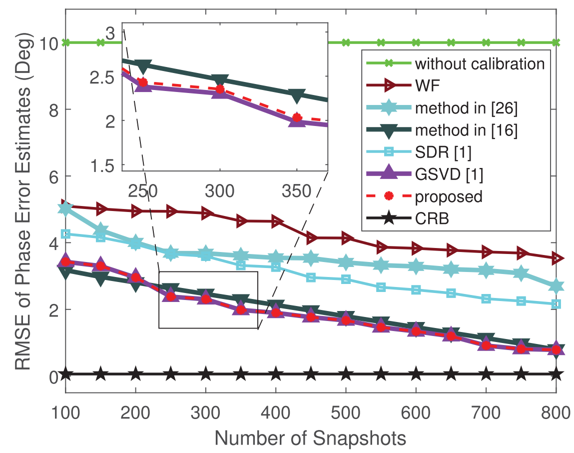

(b)

Fig. 11. RMSEs of estimates versus the number of snapshots. (a) DOA estimation. (b) Phase error estimation.

3) *Estimation Performance Versus Number of Snapshots:* In this example, we study the performance versus the number of training snapshots. Simulation results are displayed in Fig. 11, from which the strengths of the proposed method can be well verified. The GSVD method may obtain somewhat lower RMSEs than those of the proposed CCP-based method, and the resulting curves of these two methods overlap in general.

4) *Estimation Performance Versus DOA Perturbation:* To further explore the performance of the proposed method, we investigate the effect of the perturbation of DOA estimation [i.e., δ_θ in (24)]. To this end, we vary δ_θ from 2° to 20°. The resultant RMSEs of DOA and phase error estimation are displayed in Fig. 12. It is seen that the proposed approach is quite robust against the DOA perturbation, and the RMSEs are nearly not affected by δ_θ. Note that the proposed method and the GSVD method outperform other approaches tested. In addition, the GSVD approach behaves slightly better than the proposed one, and the superiority is minor. As aforementioned, the possible reason is that our method may be somewhat affected by iteration number and/or termination criterion.

TABLE III
Parameter Comparison of One Realization of Our Method Using a Fully Uncalibrated Array

	real	estimated ([20])	estimated(proposed)
ϕ_2	-17.0009°	-19.7481°	-16.8529°
ϕ_3	20.8661°	21.4789°	20.8332°
ϕ_4	-12.7796°	-13.1510°	-12.9319°
ϕ_5	-10.1301°	-12.7546°	-10.3108°
ϕ_6	37.7666°	34.4373°	37.7822°
ϕ_7	2.3357°	**2.2330°**	**2.2330°**
θ	26.0000°	26.2000°	26.0276°

C. 2-D Planar Array With Fully Uncalibrated Sensors

To further show the wide applicability of the proposed algorithm, we next consider a 2-D planar array with fully uncalibrated sensors. The array geometry follows the preceding example, see Table I and Fig. 4. Different from the previous two cases, all the sensors are uncalibrated in this example. The real orientation of calibration source is $\theta = 26^\circ$, and we know *a priori* that the DOA is located in the range $[\theta_0 - \delta_\theta, \theta_0 + \delta_\theta]$ with $\theta_0 = 24^\circ$ and $\delta_\theta = 8^\circ$. In this case, we set $\sigma_\phi = 30^\circ$, SNR = 15 dB, and $L = 400$. Table III specifies the real phase error values in one realization. Since there is no such calibrated sensor available

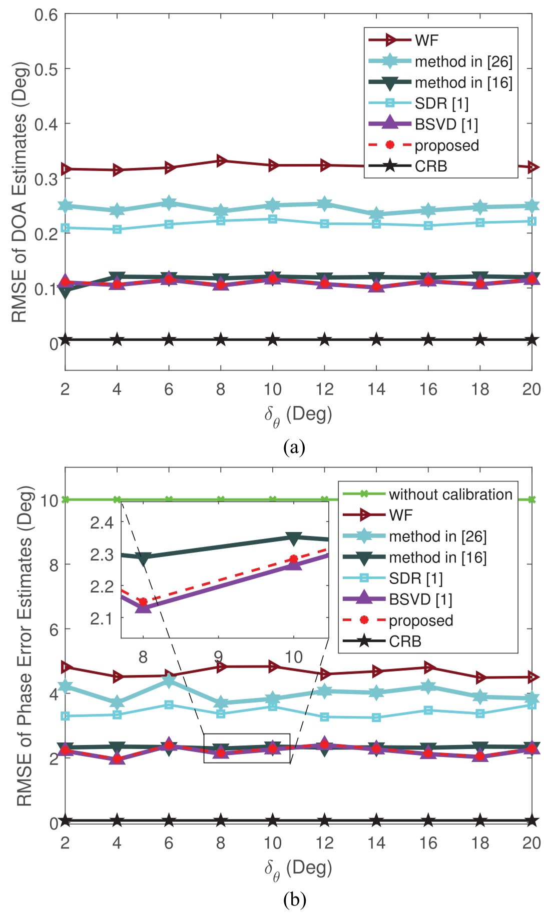

Fig. 12. RMSEs of estimates versus DOA perturbation δ_θ. (a) DOA estimation. (b) Phase error estimation.

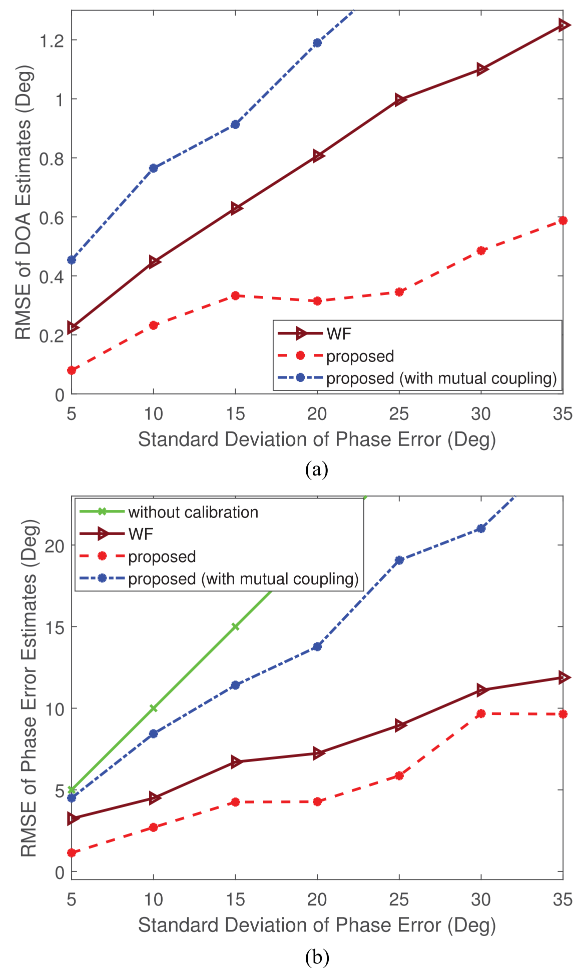

Fig. 13. RMSEs of estimates versus standard deviation of phase error using fully uncalibrated sensors. (a) DOA estimation. (b) Phase error estimation.

in the above scenario, we follow the strategy presented in Remark 3 and carry out the WF algorithm in [20] to obtain a rough estimation of DOA and phase error, see the results in Table III. Note from Table III that the estimation of ϕ_7 by WF method is 2.2330°, which has the less phase error estimation deviation (from the presumed value) among all the phase error estimations. On this basis, we select the seventh sensor as the calibrated one (i.e., set $c = 7$ and $\phi_c = 2.2330°$), and carry out our method to re-estimate the DOA and phase error. Table III summarizes the ultimate estimations of the proposed method. One can see that our estimates (including DOA and phase error) are closer to the real values than those of the WF algorithm in [20].

To further investigate the performance of our method for a fully uncalibrated array, we vary σ_ϕ from 5° to 35° and carry out Monte Carlo simulation by taking the realization number as 1000. Fig. 13 depicts the resulting RMSEs of DOA and phase error for the WF method in [20] and the proposed one. We can see that our method performs better than the WF algorithm, although the resulting RMSEs have been increased when compared to the results in Fig. 9, where a calibrated sensor is assumed. Therefore, for a fully calibrated array, the proposed algorithm also works well after simple modifications.

As we have pointed out earlier, the proposed method is failed if there exists mutual coupling between sensor elements. We next take mutual coupling error into consideration and explore the performance of our method in this scenario by varying σ_ϕ from 5° to 35°. More specifically, the mutual coupling matrix $\mathbf{C}$ is complex symmetry with unit elements on diagonal. The amplitudes of other entries of $\mathbf{C}$ are fixed as -15 dB, and their phases are distributed uniformly in the range $[0, 2\pi)$. The resulting RMSEs of DOA and phase error are shown with blue dashed lines in Fig. 13, from which we find that the performance of the proposed method has been seriously degraded compared to the case when the mutual coupling is absent. This coincides with the theoretical prediction of Remark 1.

VI. CONCLUSION

We have presented a novel strategy to simultaneously estimate the DOA of a source signal and phase error of a partly calibrated array with arbitrary geometrical configuration. We add the snapshot data of two different sensor elements together and then extract the information associated with the DOA and phase errors by carrying out SVD procedure. In such a manner, a series of linear equations with respect to the unknown DOA and phase error are further established. On this basis, it has been shown that the problem of jointly estimating DOA and phase error is equivalent to an LS problem with a quadratic equality constraint. To solve this LS problem (so that the DOA and phase error can be obtained), the CCP approach has been employed. Different from the conventional algorithms that are limited to specific array geometries, the proposed one is suitable for arrays with arbitrary geometries. More importantly, the devised method only requires one extra calibrated sensor, which is not necessarily adjacently located with the reference one. After simple modifications, our algorithm also works for the fully uncalibrated arrays. Several representative experiments have been carried out in this paper and both the effectiveness and the superiority of the proposed method have been well validated. As a future study, we may consider the DOA estimation of multiple sources in the presence of mutual coupling and/or array shape mismatch.

ACKNOWLEDGMENT

The authors would like to thank the editor and the anonymous reviewers for their valuable comments and suggestions.

REFERENCES

[1] X. Zhang, Z. He, B. Liao, J. Qian, and J. Xie
Estimation of DOA and phase error using a partly calibrated sensor array with arbitrary geometry
In *Proc. Eur. Signal Process. Conf.*, Budapest, Hungary, Sep. 2016, pp. 1916–1920.

[2] A. K. Seghouane
A Kullback-Leibler methodology for unconditional ML DOA estimation in unknown nonuniform noise
IEEE Trans. Aerosp. Electron. Syst., vol. 47, no. 4, pp. 3012–3021, Oct. 2011.

[3] C. Qian, L. Huang, M. Cao, H. C. So, and J. Xie
PUMA: An improved realization of MODE for DOA estimation
IEEE Trans. Aerosp. Electron. Syst., vol. 53, no. 5, pp. 2128–2139, Oct. 2017.

[4] N. Hu, Z. Ye, X. Xu, and M. Bao
DOA estimation for sparse array via sparse signal reconstruction
IEEE Trans. Aerosp. Electron. Syst., vol. 49, no. 2, pp. 760–773, Apr. 2013.

[5] F. Wan, W. P. Zhu, and M. N. S. Swamy
Spacial extrapolation-based blind DOA estimation approach for closely spaced sources
IEEE Trans. Aerosp. Electron. Syst., vol. 46, no. 2, pp. 569–582, Apr. 2010.

[6] B. Liao, S. C. Chan, L. Huang, and C. Guo
Iterative methods for subspace and DOA estimation in nonuniform noise
IEEE Trans. Signal Process., vol. 64, no. 12, pp. 3008–3020, Jun. 2016.

[7] R. O. Schmidt
Multiple emitter location and signal parameter estimation
IEEE Trans. Antennas Propag., vol. AP-34, no. 3, pp. 276–280, Mar. 1986.

[8] R. Roy and T. Kailath
ESPRIT-estimation of signal parameters via rotational invariance techniques
IEEE Trans. Acoust., Speech, Signal Process., vol. 37, no. 7, pp. 984–995, Jul. 1989.

[9] P. Stoica and A. Nehorai
MUSIC, maximum likelihood and Cramer-Rao bound
IEEE Trans. Acoust., Speech, Signal Process., vol. 37, no. 5, pp. 720–741, May 1989.

[10] Z. Ye, J. Dai, X. Xu, and X. Wu
DOA estimation for uniform linear array with mutual coupling
IEEE Trans. Aerosp. Electron. Syst., vol. 45, no. 1, pp. 280–288, Jan. 2009.

[11] F. Li and R. J. Vaccaro
Sensitivity analysis of DOA estimation algorithms to sensor errors
IEEE Trans. Aerosp. Electron. Syst., vol. 28, no. 3, pp. 708–717, Jul. 1992.

[12] X. Zhang, Z. He, B. Liao, X. Zhang, Z. Cheng, and Y. Lu
A^2RC: An accurate array response control algorithm for pattern synthesis
IEEE Trans. Signal Process., vol. 65, no. 7, pp. 1810–1824, Apr. 2017.

[13] B. Friedlander and A. J. Weiss
Direction finding in the presence of mutual coupling
IEEE Trans. Antennas Propag., vol. 39, no. 3, pp. 273–284, Mar. 1991.

[14] F. Sellone and A. Serra
A novel online mutual coupling compensation algorithm for uniform and linear arrays
IEEE Trans. Signal Process., vol. 55, no. 2, pp. 560–573, Feb. 2007.

[15] B. Liao, Z. G. Zhang, and S. C. Chan
DOA estimation and tracking of ULAs with mutual coupling
IEEE Trans. Aerosp. Electron. Syst., vol. 48, no. 1, pp. 891–905, Jan. 2012.

[16] J. Pierre and M. Kaveh
Experimental performance of calibration and direction-finding algorithms
In *Proc. IEEE Int. Conf. Acoust., Speech, Signal Process.*, 1991, pp. 1365–1368.

[17] H. S. Mir
A generalized transfer-function based array calibration technique for direction finding
IEEE Trans. Signal Process., vol. 56, no. 2, pp. 851–855, Feb. 2008.

[18] H. S. Mir and J. D. Sahr
Passive direction finding using airborne vector sensors in the presence of manifold perturbations
IEEE Trans. Signal Process., vol. 55, no. 1, pp. 156–164, Jan. 2007.

[19] H. S. Mir, J. D. Sahr, G. F. Hatke, and C. M. Keller
Passive source localization using an airborne sensor array in the presence of manifold perturbations
IEEE Trans. Signal Process., vol. 55, no. 6, pp. 2486–2496, Jun. 2007.

[20] B. Friedlander and A. J. Weiss
Eigenstructure methods for direction finding with sensor gain and phase uncertainties
In *Proc. IEEE Int. Conf. Acoust., Speech, Signal Process.*, Apr. 1988, pp. 2681–2684.

[21] A. Liu, G. Liao, C. Zeng, Z. Yang, and Q. Xu
An eigenstructure method for estimating DOA and sensor gain-phase errors
IEEE Trans. Signal Process., vol. 59, no. 12, pp. 5944–5956, Dec. 2011.

[22] S. Cao, Z. Ye, D. Xu, and X. Xu
A Hadamard product based method for DOA estimation and gain-phase error calibration
IEEE Trans. Aerosp. Electron. Syst., vol. 49, no. 2, pp. 1224–1233, Apr. 2013.

[23] N. Boon Chong and S. Chong Meng Samson
Sensor-array calibration using a maximum-likelihood approach
IEEE Trans. Antennas Propag., vol. 44, no. 6, pp. 827–835, Jun. 1996.

[24] W. Wang, R. Wu, J. Liang, and H. C. So
Phase retrieval approach for DOA estimation with array errors
IEEE Trans. Aerosp. Electron. Syst., vol. 53, no. 5, pp. 2610–2620, Oct. 2017.

[25] M. Viberg and A. L. Swindlehurst
A Bayesian approach to auto-calibration for parametric array signal processing
IEEE Trans. Signal Process., vol. 42, no. 12, pp. 3495–3507, Dec. 1994.

[26] V. C. Soon, L. Tong, Y. F. Huang, and R. Liu
A subspace method for estimating sensor gains and phases
IEEE Trans. Signal Process., vol. 42, no. 4, pp. 973–976, Apr. 1994.

[27] B. P. Ng, J. P. Lie, M. H. Er, and A. Feng
A practical simple geometry and gain/phase calibration technique for antenna array processing
IEEE Trans. Antennas Propag., vol. 57, no. 7, pp. 1963–1972, Jul. 2009.

[28] J. Liu, X. Wu, W. J. Emery, L. Zhang, C. Li, and K. Ma
Direction-of-arrival estimation and sensor array error calibration based on blind signal separation
IEEE Signal Process. Lett., vol. 24, no. 1, pp. 7–11, Jan. 2017.

[29] A. Paulraj and T. Kailath
Direction of arrival estimation by eigenstructure methods with unknown sensor gain and phase
In *Proc. IEEE Int. Conf. Acoust., Speech, Signal Process.*, 1985, pp. 640–643.

[30] Y. Li and M. H. Er
Theoretical analyses of gain and phase error calibration with optimal implementation for linear equispaced array
IEEE Trans. Signal Process., vol. 54, no. 2, pp. 712–723, Feb. 2006.

[31] M. P. Wylie, S. Roy, and H. Messer
Joint DOA estimation and phase calibration of linear equispaced (LES) arrays
IEEE Trans. Signal Process., vol. 42, no. 12, pp. 3449–3459, Dec. 1994.

[32] K. Han, P. Yang, and A. Nehorai
Calibrating nested sensor arrays with model errors
IEEE Trans. Antennas Propag., vol. 63, no. 11, pp. 4739–4748, Nov. 2015.

[33] M. Pesavento, A. B. Gershman, and K. M. Wong
Direction finding in partly calibrated sensor arrays composed of multiple subarrays
IEEE Trans. Signal Process., vol. 50, no. 9, pp. 2103–2115, Sep. 2002.

[34] M. Li and Y. Lu
Source bearing and steering-vector estimation using partially calibrated arrays
IEEE Trans. Aerosp. Electron. Syst., vol. 45, no. 4, pp. 1361–1372, Oct. 2009.

[35] L. Lei, J. P. Lie, A. B. Gershman, and M. S. S. Chong
Robust adaptive beamforming in partly calibrated sparse sensor arrays
IEEE Trans. Signal Process., vol. 58, no. 3, pp. 1661–1667, Mar. 2010.

[36] C. M. S. See and A. B. Gershman
Direction-of-arrival estimation in partly calibrated subarray-based sensor arrays
IEEE Trans. Signal Process., vol. 52, no. 2, pp. 329–338, Feb. 2004.

[37] B. Liao and S. C. Chan
Direction finding with partly calibrated uniform linear arrays
IEEE Trans. Antennas Propag., vol. 60, no. 2, pp. 922–929, Feb. 2012.

[38] B. Liao and S. C. Chan
Direction finding in partly calibrated uniform linear arrays with unknown gains and phases
IEEE Trans. Aerosp. Electron. Syst., vol. 51, no. 1, pp. 217–227, Jan. 2015.

[39] B. Liao, J. Wen, L. Huang, C. Guo, and S. C. Chan
Direction finding with partly calibrated uniform linear arrays in nonuniform noise
IEEE Sensors J., vol. 16, no. 12, pp. 4882–4890, Jun. 2016.

[40] T. Lipp and S. Boyd
Variations and extension of the convex–concave procedure
Optim. Eng., vol. 17, pp. 263–287, 2016.

[41] J. Capon
High-resolution frequency-wavenumber spectrum analysis
Proc. IEEE, vol. 57, no. 8, pp. 1408–1418, Aug. 1969.

[42] W. Gander
Least squares with a quadratic constraint
Numerische Mathematik, vol. 36, pp. 291–307, 1981.

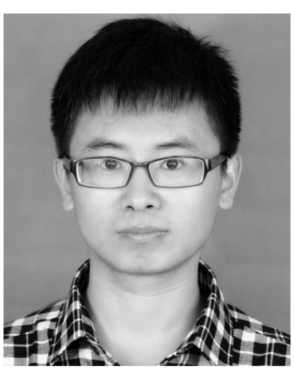

Xuejing Zhang (S'17) was born in Hebei Province, China. He received the B.S. degree in electrical engineering from Huaqiao University, Xiamen, China, in 2011, and the M.S. degree in signal and information processing from Xidian University, Xi'an, China, in 2014. He is currently working toward the Ph.D. degree in signal and information processing at the School of Information and Communication Engineering, University of Electronic Science and Technology of China, Chengdu, China.

Since November 2017, he has been a Visiting Student with the University of Delaware, Newark, DE, USA. His research interests include array signal processing and wireless communications.

Zishu He (M'11) was born in Sichuan Province, China, in 1962. He received the B.S., M.S., and Ph.D. degrees in signal and information processing from the University of Electronic Science and Technology of China (UESTC), Chengdu, China, in 1984, 1988, and 2000, respectively.

He is currently a Professor with the School of Information and Communication Engineering, UESTC. His research interests include array signal processing, digital beam forming, the theory on multiple-input multiple-output (MIMO) communication and MIMO radar, adaptive signal processing, and interference cancelation.

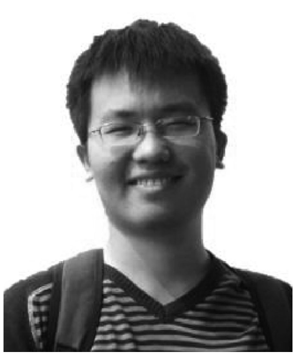

Xuepan Zhang was born in Hebei Province, China. He received the B.S. degree from Xidian University, Xi'an, China, in 2010, and the Ph.D. degree from the National Laboratory of Radar Signal Processing, Xi'an, China, in 2015, both in electrical engineering.

He is currently a Principal Investigator with the Qian Xuesen Laboratory of Space Technology, Beijing, China. His research interests include synthetic aperture radar, ground moving target indication, and deep learning.

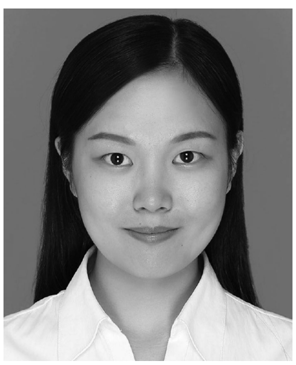

Yue Yang (S'17) was born in Sichuan Province, China. She received the B.Eng. degree in electronic engineering from the University of Electronic Science and Technology of China (UESTC), Chengdu, China, in 2015. She is currently working toward the Ph.D. degree in signal and information processing at the School of Information and Communication Engineering, UESTC.

Since January 2019, she has been a Visiting Student with the National University of Singapore, Singapore. Her research interests include synthetic aperture radar imaging, sparse signal reconstruction, and statistical signal processing.